Communication

Chemically Induced Solidification: A New Way to Produce Thin Solid-Near-Net Shapes

CARL SLATER, STEPHEN SPOONER, CLAIRE DAVIS, and SEETHARAMAN SRIDHAR

In situ observation of the solidification of high-carbon steel (4 wt pct C) through decarburization has been carried out as a feasibility study into reducing high-power usage and high CO_2 production involved in steel making. Decarburization has been carried out under both air and pure N_2 atmospheres at temperatures of 1573 K and 1673 K (1300 °C and 1400 °C). A solidified shell of around 500 μm was formed with carbon concentrations reduced down to 1 pct in as short as 18 seconds.

DOI: 10.1007/s11663-016-0785-8

In 2012, Park *et al.*[1] suggested the feasibility of decarburizing 4 wt pct C cast iron in solid state during the continuous strip casting process using oxidizing gases (such as CO_2 and H_2O), called the S^3 process. The advantage of such a process would be that aspects of the steelmaking process, such as the basic oxygen furnace (BOF), can be circumvented, therefore avoiding large amounts of oxygen and unwanted oxide inclusion products. Although the results showed promise, decarburization rates to 0.5 wt pct were in excess of 30 minutes for a 1-mm strip. Later the S^3-II[2] process was proposed where some decarburization occurs in the tundish (down to 1.2–1.9 wt pct) by bubbling O_2 before further solid state decarburization. Decarburizing to this point in the liquid ensures no excess oxygen to form oxides and, thus, still achieves "clean" steel production. This reduced solid state decarburization decreases the time to around 10 minutes for 1-mm strips held at 1473 K (1200 °C).

Belt casting (particularly horizontal single belt casting (HSBC)) offers the unique possibility of introducing gases during the solidification of steel and affects the steel chemistry through the strip thickness thanks to the thin cross section. This opens up the possibility of expanding on the premise of the S^3-II process and of decarburizing to a lower carbon fraction in the liquid to the point of solidification (a limit not desirable to attain in the tundish). Therefore, the aim of this work is to understand and observe the isothermal solidification of liquid iron similar in composition to pig iron by means of decarburization in both air and N_2 atmospheres. This therefore explores the feasibility of an inline continuous decarburizing and non-CO_2 forming (in the case of N_2) method of producing steel while allowing for a different solidification structure. The limit of decarburization in this case may be the balance between the desirable removal of carbon and the undesirable dissolution of interstitials (oxygen and nitrogen) and the formation of oxides (and other such undesirably products of interaction with these gases).

A high-temperature confocal scanning laser microscope (CSLM) was used to observe the *in situ* solidification of the molten steel (an outline of the CSLM technique has been covered in a previous paper[3]). A Fe-4C-0.2P steel was used for this study, and samples were machined to cubes of around 0.25 g. The purpose of phosphorous addition was to enable the solidification structure to be revealed. The samples were heated at 10 K/s to a set peak temperature under argon (with and O_2 concentration <2 ppm and a flow rate of 200 mL/min), and after a 15-seconds hold, the atmosphere was switched to a decarburizing atmosphere (either air or N_2) at a slow rate of 100 mL/min. As decarburization occurs, the sample travels along the depicted line in Figure 1 until solidification of the observable surface appeared to be completed, after which the atmosphere was switched immediately back to Ar before cooling to room temperature (at a rate of 1 K/s). The time taken for replacing the gas atmosphere in the chamber twice is estimated to be 30 seconds and is described in the previous works.[3]

Figure 1 shows an example time lapse of the solidification of the pig iron under an air atmosphere at 1573 K (1300 °C). It can be seen that three distinct phases are present: liquid, austenite (as indicated by the first solid phase appearing in the pathways shown in Figure 1), and a particulate (which appears almost instantly once the atmosphere changes). The particulate phase has been proven to be carbon enriched through SEM-EDS mapping (an intensity of over 10 times that seen in the bulk material) of several particle examples found on the surface of a test sample quenched in a nitrogen atmosphere as soon as the particulate phase formed. The sample was taken straight to SEM to avoid contamination, and multiple scans of the same area were conducted to remove the possibility of carbon deposition during analysis being the cause of detection; the phase showed a depletion in oxygen compared to the main matrix, removing the possibility of this being oxide formation. Figure 2 shows the phase distribution of the

CARL SLATER, Research Fellow, STEPHEN SPOONER, Ph.D. Student, CLAIRE DAVIS, Professor, and SEETHARAMAN SRIDHAR, Professor, are with WMG, University of Warwick, Coventry, U.K. Contact e-mail: c.d.slater@warwick.ac.uk.
Manuscript submitted June 27, 2016.
Article published online September 26, 2016.

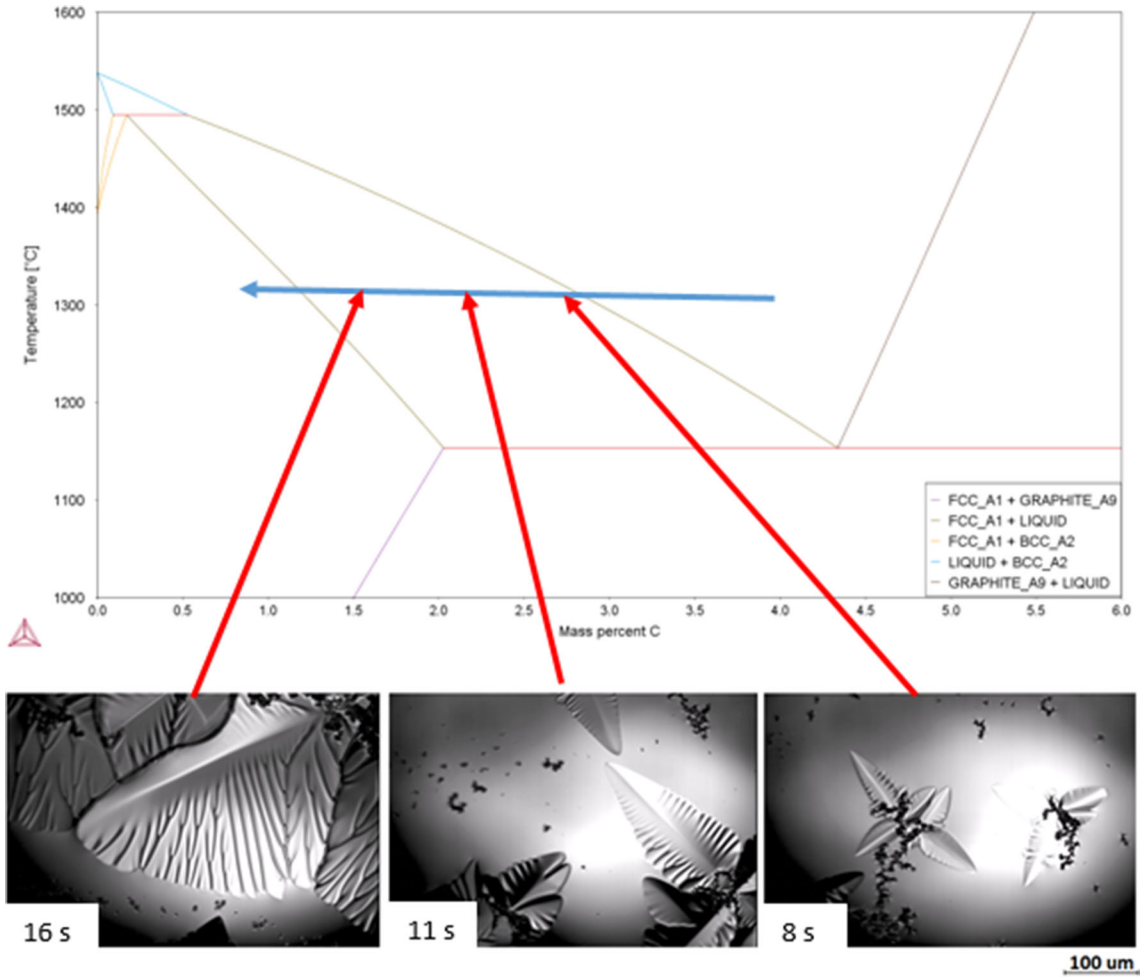

Fig. 1—Fe-C phase diagram showing the path of solidification through decarburization (blue) and time lapse image showing the solidification through decarburization (from right to left) in air at 1573 K (1300 °C) (with times related to the point of gas switch over) (Color figure online).

system with varying N content. It is clearly seen that as mass percent of N in the liquid steel increases beyond 1 wt pct, the formation of graphite occurs under equilibrium conditions. This is possible if we consider the interaction between nitrogen and the surface of the steel as its own system (as it is this interface where the graphite is shown to form).[3]

A summary of the critical points of the solidification process can be seen in Table I for all the conditions assessed. For the conditions in air, a clear increase in the time to first solid was seen with increasing temperature; however, the time from first solid to last liquid (transformation time) decreased with temperature. These trends are consistent with the phase diagram where at higher temperatures more carbon needs to be removed to start solidification. Nevertheless, the mushy zone width is much narrower than it is at lower temperatures.

Decarburization with oxygen in the air forms a mixture of CO and CO_2. These molecules will form a boundary layer at the surface of the metal if the production of CO/CO_2 is greater than the diffusion of the gases away from the surface.[4] Previous reports by Sain[5] and Fruehan[6] indicate that the interfacial reaction between oxygen and carbon is very fast and gas molecule sticking parameters are very low (step 5) at these temperatures. Mass transfer in the bulk phases have been reported to be slower and, therefore, are likely to be rate controlling. Of these mass transports, it is O_2 diffusion through the boundary layer that is likely the dominant rate controlling factor due to the low driving force of oxygen through this layer. This is supported in levitated droplet experiments[7,8] where swelling is observed and discussion of limited diffusion of the reactant gases away from the interface is the given reasoning.

In the case of nitrogen, the reaction produces a combination of C_2N_2 (cyanogen) and XCN (variable cyanides) and the reaction steps are similar to that of decarburization with air; however, following the reported rates of nitrogen absorption into the melt,[9] the rate of decarburization required for the viewed solidification in nitrogen would not be possible. As such it is suggested that decarburization with nitrogen is dominated through the pathway of either atomic or diatomic nitrogen reaction with precipitated carbon-enriched particulate phase. Decarburization by nitrogen reaction with graphite is further supported by the observed retardation of the reaction at higher temperatures. Previous findings[10] report the reduced reaction rate of graphite and nitrogen at higher temperatures due

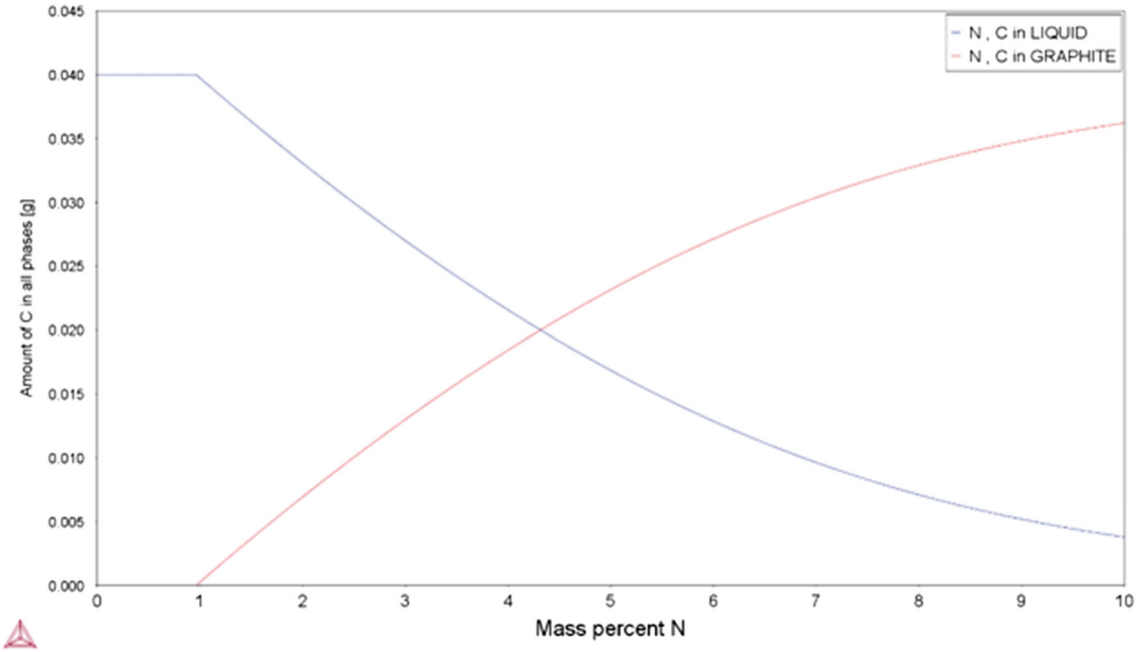

Fig. 2—Thermocalc prediction showing the stabilization of graphite in the presence of N.

Table I. Summary of the Time Taken for First Solid and Last Liquid to Occur Under Different Atmospheric Conditions

Temperature K (°C)	Atmosphere*	Time to First Solid (s)	Time to Last Liquid (s)	Transformation Time (s)
1573 (1300)	argon	not observed	not observed	—
1673 (1400)	argon	not observed	not observed	—
1773 (1500)	argon	not observed	not observed	—
1573 (1300)	air	7	18	11
1673 (1400)	air	11	18	7
1773 (1500)	air	34	39	4
1573 (1300)	N2	32	155	123
1673 (1400)	N2	not observed	not observed	—
1673 (1400)	N2 (increased rate of 400 mL/min)	265	841	576

*All tests were carried out with an atmospheric flow rate of 100 mL/min unless otherwise stated.

to the rate of graphite ''healing'' being increased more than the rate of gasification with temperature (where the balance between reactant and products moves to reduce the rate of decarburization). In the case of nitrogen, no noticeable surface contamination (such as the oxide layer seen in air) was observed, suggesting that postsolidification decarburization can continue under this atmosphere (although the rate-limiting steps may change).

Figure 3(a) shows the as-cast microstructure of the high-carbon iron used in this study that has been melted and resolidified in argon. A solidified dendritic structure can be seen. These dendrites form as austenite and on further cooling transform to pearlite. Although the interdendritic regions are enriched in carbon, subsequently graphite can be seen in a ferrite matrix. The samples where decarburization has occurred showed a decarburized shell (consistently around 300–500 μm thick; Figure 3(b)), and micrographs of this shell can be seen in Figures 3(c) through (e). Here pro-eutectoid cementite can be seen in a pearlite matrix. Based on the level of cementite (area percent values of 11.7, 3.3, and 15.4 for Figures 3(c) through (e), respectively), then the amount of carbon in this region can be calculated by the lever rule to be 1.48, 0.99, and 1.7 wt pct, respectively.

The results shown here suggest that the feasibility of decarburization of high-carbon steel can be achieved down to lower carbon levels than the S^3 process and in a shorter period of time while the steel is liquid. Particularly under a N2 atmosphere, samples with around a 0.5-mm decarburized layer (between 1 and 1.7 wt pct carbon remaining) were produced with very little/no observable contamination on the surface. This suggests that this is a ''clean'' method of decarburizing steel that can be implemented inline of the continuous casting process, while having the potential of bypassing certain steelmaking processes such as the BOF. The results also suggest that a layered microstructure can be achieved and layer thicknesses potentially controlled by the duration of gas exposure conditions (flow rate and gas chemistry).

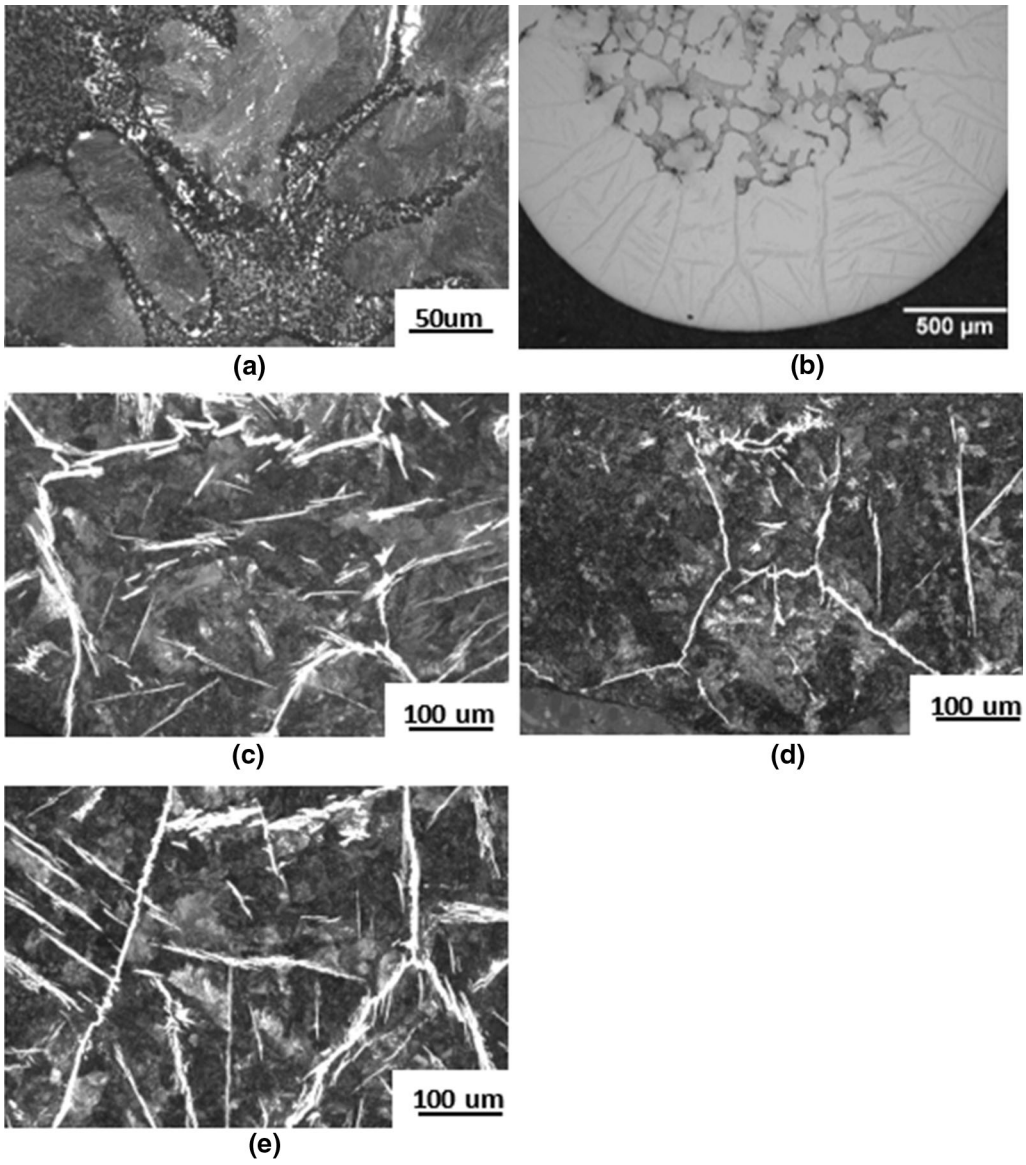

Fig. 3—Micrographs of samples etched in 3 pct Nital (*a*) pig iron cast in argon, (*b*) an unetched sample showed the solidified shell, (*c*) decarburized at 1573 K (1300 °C) in air, (*d*) decarburized at 1573 K (1300 °C) in N, and (*e*) decarburized at 1673 K (1400 °C) in N.

The authors would like to thank EPSRC for funding (Grant Number EP/M014002/1) and WMG for their support and facilities.

REFERENCES

1. J. Park, T. Van Long, and Y. Sasaki: *Tetsu-to-Hagané*, 2012, vol. 98, pp. 26–34.
2. W.-H. Lee, J.-O. Park, J.-S. Lee, J.A. de Castro, and Y. Sasaki: *Ironmak. Steelmak.*, 2012, vol. 39, pp. 530–34.
3. C. Slater, S. Spooner, C. Davis, and S. Sridhar: *Mater. Lett.*, 2016, vol. 173, pp. 98–101.
4. H. Schliching: *Boundry-Layer Theory*, 7th ed., McGraw-Hill, New York, 1979, p. 535.
5. D.R. Sain and G.R. Belton: *Metall. Mater. Trans. B*, 1976, vol. 7B, pp. 235–44.
6. R.J. Fruehan and L.J. Martonik: *Metall. Mater. Trans. B*, 1974, vol. 5B, pp. 1027–32.
7. E. Chen and K.S. Coley: *Ironmak. Steelmak.*, 2010, vol. 37, pp. 541–45.
8. C. Molloseau and R. Fruehan: *Metall. Mater. Trans. B*, 2002, vol. 33B, pp. 335–44.
9. R.J. Fruehan and L.J. Martonik: *Metall. Trans. B*, 1980, vol. 11B, pp. 615–21.
10. C.F. Cullis and J.G. Yates: *Trans. Faraday Soc.*, 1964, vol. 60, pp. 141–48.